ARTICLES

Low-Lying Electronic States and Cl-Loss Photodissociation of the $C_2H_3Cl^+$ Ion Studied Using Multiconfiguration Second-Order Perturbation Theory

Hai-Bo Chang, Bo-Zhen Chen,* and Ming-Bao Huang*

College of Chemistry and Chemical Engineering, Graduate University of Chinese Academy of Sciences, P.O. Box 4588, Beijing 100049, People's Republic of China

Received: November 6, 2007; In Final Form: December 10, 2007

We studied the $1^2A''(X^2A'')$, $1^2A'$ (A^2A'), $2^2A''$ (B^2A''), and $2^2A'$ (C^2A') states of the $C_2H_3Cl^+$ ion using the complete active space self-consistent field (CASSCF) and multiconfiguration second-order perturbation theory (CASPT2) methods. For the four ionic states, we calculated the equilibrium geometries, adiabatic (T_0) and vertical (T_v) excitation energies, and relative energies (T_v') at the geometry of the molecule at the CASPT2 level and the Cl-loss dissociation potential energy curves (PECs) at the CASPT2//CASSCF level. The computed oscillator strength f value for the $X^2A'' \leftarrow A^2A'$ transition is very small, which is in line with the experimental fact that the A state has a long lifetime. The CASPT2 geometry and T_0 value for the A^2A' state are in good agreement with experiment. The CASPT2 T_v' values for the A^2A', B^2A'', and C^2A' states are in good agreement with experiment. The Cl-loss PEC calculations predict that the X^2A'', A^2A', and C^2A' states correlate to $C_2H_3^+$ (X^1A_1) and the B^2A'' state to $C_2H_3^+$ ($1^3A''$) (the B^2A'' and C^2A' PECs cross at $R(C-Cl) \approx 2.24$ Å). Our calculations indicate that at 357 nm the X^2A'' state can undergo a transition to B^2A'' followed by a predissociation of B^2A'' by the repulsive C^2A' state (via the B/C crossing), leading to $C_2H_3^+$ (X^1A_1), and therefore confirm the experimentally proposed pathway for the photodissociation of X^2A'' at 357 nm. Our CASPT2 D_0 calculations support the experimental fact that the X state does not undergo dissociation in the visible spectral region and imply that a direct dissociation of the A state to $C_2H_3^+$ (X^1A_1) is energetically feasible.

Introduction

Since 2000, Kim et al. detected long-lived excited electronic states for a number of molecular ions, including the benzene ion (the B^2E_{2g} state),[1] monosubstituted benzene ions ($C_6H_5X^+$, X = Cl, Br, CN, and C≡CH; the B^2B_2 states),[2] and monosubstituted ethene ions ($C_2H_3X^+$, X = Cl, Br, I, and CN; the A^2A' states),[3] by using the charge exchange technique. Among these molecular ions, the vinyl chloride ion ($C_2H_3Cl^+$) is the smallest.

After their detection of the long-lived A state of the $C_2H_3Cl^+$ ion, Kim et al.[4] studied properties of the A state using one-photon mass-analyzed threshold ionization (MATI) spectroscopy and reported the vertical ionization energy (11.67 eV) and geometry of the A state. They[5] also studied photodissociation of the $C_2H_3Cl^+$ ion in the X and A states using mass-analyzed ion kinetic energy spectrometry (MIKES). They[5] proposed that at 357 nm the X state could undergo a transition to the B state followed by a predissociation of B by the C state leading to $C_2H_3^+$ and that the C ← A optical transition was responsible for the photodissociation processes of the A state. They[5] reported that the X state did not undergo dissociation in the visible spectral region.

We have carried out high-level ab initio calculations for the low-lying electronic states of the $C_2H_3Cl^+$ ion, and in the present article we will report our calculation results concerning properties and Cl-loss dissociation processes of the low-lying states and discuss these results in comparison with the experimental results reported recently by Kim et al.[3−5] and previously by other groups (see below).

It is already known[3,5−9] that the X, A, B, and C states of the $C_2H_3Cl^+$ ion are $1^2A''$, $1^2A'$, $2^2A''$, and $2^2A'$, respectively. Experimental vertical ionization energies (VIEs) for the four states of $C_2H_3Cl^+$ were already reported by many groups.[3−4,6−16] On the basis of the experimental VIE values for different states of the ion, relative energy values (denoted by T_v' in the present paper) of the excited states to the ground state of the ion at the ground-state geometry of the neutral molecule can be evaluated. Using the experimental VIE values for the X, A, B, and C states (10.18, 11.72, 13.14, and 13.56 eV, respectively) reported by Lake and Thompson,[6] the T_v' values for the $1^2A'$, $2^2A''$, and $2^2A'$ states are evaluated to be 1.54, 2.96, and 3.38 eV, respectively. Using the experimental VIE values for the X, A, B, and C states (10.005, 11.664, 13.13, and 13.56 eV, respectively) reported by Locht et al.,[7] the T_v' values for the $1^2A'$, $2^2A''$, and $2^2A'$ states are evaluated to be 1.66, 3.13, and 3.56 eV, respectively. Experimental adiabatic ionization energies (AIEs) for the X and A states of $C_2H_3Cl^+$ were reported by Lake and Thompson.[6] On the basis of the experimental AIE values for different states of the ion, adiabatic excitation energies (denoted by T_0 in the present paper) of the excited states can be evaluated. Using the reported experimental AIE values for

* Corresponding author. E-mail for M.-B.H.: mbhuang1@gucas.ac.cn.

10.1021/jp710633s CCC: $40.75
Published on Web 02/02/2008

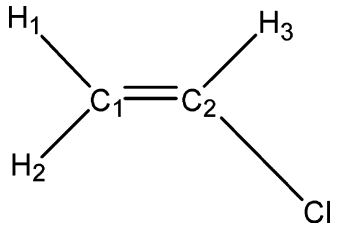

Figure 1. Atom labelings for the $C_2H_3Cl^+$ ion (C_s) used in the present work.

the X and A states (10.00 and 11.72 eV, respectively),[6] the T_0 value for the $1^2A'$ state is evaluated to be 1.72 eV.

The experimental geometry of the A state of $C_2H_3Cl^+$ was reported by Kim et al.,[4] and we found no reported experimental geometries for the other three states in the literature. Photodissociation studies for the $C_2H_3Cl^+$ ion were carried out by several groups,[5,11−13,17,18] and the observed products and the measured dissociation energies and appearance energies were reported.

In their experimental papers[3−5] Kim et al. also reported theoretical calculation results for the excited states of $C_2H_3Cl^+$, and their calculations were performed using the TDDFT/B3LYP method. In the present theoretical study on the $1^2A''$, $1^2A'$, $2^2A''$, and $2^2A'$ states of the $C_2H_3Cl^+$ ion, the complete active space self-consistent-field (CASSCF)[19] and multiconfiguration second-order perturbation theory (CASPT2)[20,21] methods were used. These methods are considered to be effective for theoretical studies (on equilibrium geometries, energetics, dissociation processes, and other properties) of the excited electronic states of molecules and molecular ions.

Calculation Details

Geometry and atom labelings used for the $C_2H_3Cl^+$ ion are shown in Figure 1. In the calculations for Cl-loss dissociation processes from the four C_s states ($1^2A''$, $1^2A'$, $2^2A''$, and $2^2A'$), we assume that the $C_2H_3Cl^+$ system remains in the C_s symmetry.

The CASSCF and CASPT2 calculations were carried out using the MOLCAS v5.4 and MOLCAS v6.2 quantum-chemistry software.[22,23] With a CASSCF wave function constituting the reference function, the CASPT2 calculations were performed to compute the first-order wavefunction and the second-order energy in the full-space. A contracted atomic natural orbital (ANO) basis set,[24−26] Cl[6s4p3d1f]/C[5s3p2d1f]/H[3s2p1d], was used. In our CAS calculations, 13 electrons were active and the active space included 11 orbitals [denoted as CAS (13,11)]. As in our previous CAS studies on electronic states of molecular ions,[27−30] the choice of the active space stemmed from the electron configuration of the ground-state C_2H_3Cl molecule: [...$(9a')^2(10a')^2(11a')^2(12a')^2(2a'')^2(13a')^2(3a'')^2(14a')^0(15a')^0(16a')^0(4a'')^0$...] (based on the HF/6-3ll+G(d,p) calculations). All the eleven orbitals (seven occupied plus four virtual) listed in the above square bracket were taken as active orbitals, and the chosen active space should be large enough for the CAS calculations of the lowest-lying two $^2A'$ and two $^2A''$ states of the ion. In the CASPT2 calculations, the weight values of the CASSCF reference functions in the first-order wave functions were larger than 0.87.

Geometry optimization calculations were performed for the four states of the ion at both the CASSCF and CASPT2 levels, and frequency analysis calculations were performed at the CASSCF level (at the CASSCF optimized geometries). On the basis of the CASPT2 geometry optimization calculations for the ground and (three) excited states, we obtained the CASPT2 adiabatic excitation energies (T_0) for the excited states. On the basis of the CASPT2 energy calculations for the four states at the CASPT2 optimized geometry of the ground state of the ion, we obtained the CASPT2 vertical excitation energies (T_v) for the excited states. On the basis of the CASPT2 energy calculations for the four states at the experimental ground-state geometry of the neutral molecule, we obtained the CASPT2 relative energies (T_v', see Introduction) for the excited states to the ground state of the ion. In the present article, the evaluated energy differences are not corrected for zero-point vibrational energies.

Potential energy curves (PECs) for Cl-loss dissociation from the four states of the $C_2H_3Cl^+$ ion were calculated at the CASPT2//CASSCF level. At a set of fixed $R(C_2-Cl)$ (the C_2-Cl bond distance, see Figure 1) values ranging from the C_2-Cl bond length values in the CASSCF optimized geometries of the respective states to 4.5 Å [the staring $R(C_2-Cl)$ value being 2.0 Å for the repulsive $2^2A'$ state (see below)], the CASSCF partial geometry optimization calculations were performed for the four states and then the CASPT2 energies were calculated at the four sets of the partially optimized geometries. On the basis of these calculations, the CASPT2//CASSCF Cl-loss dissociation PECs for the $1^2A''$, $1^2A'$, $2^2A''$, and $2^2A'$ states of the $C_2H_3Cl^+$ ion were obtained. The $C_2H_3Cl^+$ systems in the four states at the $R(C_2-Cl)$ value of 4.5 Å will be called as dissociation asymptote products of the respective states in the present article.

Results and Discussion

CASPT2 Optimized Geometries for the X^2A'', $1^2A'$, and $2^2A''$ States. In Table 1 given are the CASPT2 optimized geometries for the $1^2A''$ (X^2A''), $1^2A'$, and $2^2A''$ states of the $C_2H_3Cl^+$ ion and for the $1^1A'$ (X^1A') state of the C_2H_3Cl molecule. Our geometry optimization calculations indicate that the $2^2A'$ state is repulsive about the C_2-Cl bond. The CASSCF optimized geometries of the $1^2A''$, $1^2A'$, and $2^2A''$ states of the ion (very similar to the respective CASPT2 geometries, except that the CASSCF C_2-Cl bond length values are about 0.09 Å larger than the respective CASPT2 values in the $1^2A'$ and $2^2A''$ geometries) are not reported in Table 1 (given in the Supporting Information), and they will be the "starting points" of the CASPT2//CASSCF Cl-loss PECs (see below). The CASSCF frequency analysis calculations indicate that the CASSCF geometries of the $1^2A''$ and $1^2A'$ states correspond to energy minima and then the optimized geometries are the predicted equilibrium geometries. The CASSCF frequency calculations for the $2^2A''$ state produced a unique imaginary frequency (i398 cm^{-1}) of the a″ symmetry. We performed the CASPT2 energetic calculations for a few of C_1 (nonplanar) geometries (obtained by slightly distorting the CASPT2 C_s optimized geometry of the $2^2A''$ state according to the a″ vibration mode) in the 3^2A ($2^2A'' = 3^2A$) state, and the calculated energies are slightly higher than the CASPT2 energy of the C_s geometry of the $2^2A''$ state. This fact indicates that the CASSCF frequency calculations for $2^2A''$ erroneously produced the imaginary frequency (as in some other cases[31,32]) and implies that the CASPT2 C_s geometry of the $2^2A''$ state corresponds to energy minimum (in the CASPT2 potential energy surface).

Experimental geometric data (listed in Table 1) are available for the $1^2A'$ (A^2A') state of the $C_2H_3Cl^+$ ion[4] and for the $1^1A'$ (X^1A') state of the C_2H_3Cl molecule.[33] The CASPT2 geometry for the $1^2A'$ state of $C_2H_3Cl^+$ is in good agreement with the experimental geometry[4] (the deviations being not larger than 0.012 Å for the C−C and C−Cl bond lengths and being not larger than 1.5° for all the bond angles). The $1^2A'$ geometry obtained in the TDDFT/B3LYP calculations[4] is also given in

TABLE 1: CASPT2 Optimized Geometries for the X^2A'', $1^2A'$, and $2^2A''$ States[a] of the $C_2H_3Cl^+$ Ion and the X^1A' State of the C_2H_3Cl Molecule, Together with the Available Experimental Geometries and the Previously Reported TDDFT Geometries (Bond Lengths in Å and Angles in Degrees; for Atom Labelings in Figure 1)

	method	$R(C_1-C_2)$	$R(C_2-Cl)$	$\angle C_2C_1H_1$	$\angle C_2C_1H_2$	$\angle C_1C_2H_3$	$\angle C_1C_2Cl$
X^2A''	CASPT2	1.391	1.640	119.2	120.9	122.6	121.2
$1^2A'$	CASPT2	1.327	1.752	116.5	124.5	131.2	120.6
	TDDFT[b]	1.323	1.755	117.2	124.4	127.9	125.1
	exptl[c]	1.339	1.762	117.4	123.0	129.7	120.4
$2^2A''$	CASPT2	1.354	1.937	116.6	123.9	131.4	120.7
X^1A' [d]	CASPT2	1.332	1.719	118.9	122.0	123.6	123.2
	exptl[e]	1.332	1.726	119.5	121.0	123.8	122.3

[a] Our geometry optimization calculations indicate that the $2^2A'$ state of $C_2H_3Cl^+$ is repulsive. [b] The previously reported TDDFT calculations, ref 4. [c] Reference 4. [d] The ground state of the C_2H_3Cl molecule. [e] Reference 33.

Table 1. It is noted that the $C_1C_2H_3$ and C_1C_2Cl bond angle values in the TDDFT/B3LYP geometry are somewhat different from the respective values in the CASPT2 geometry, and the CASPT2 calculations predict a more accurate C_1C_2Cl bond angle value than the TDDFT/B3LYP calculations.[4] The CASPT2 geometry for the $1^1A'$ state of C_2H_3Cl is in very good agreement with the experimental geometry[33] (the deviations being smaller than 0.01 Å for the C−C and C−Cl bond lengths and being not larger than 1° for all the bond angles).

On the basis of the CASPT2 results reported in Table 1, we will preliminarily explain the geometric changes in the three ionic states (upon ionization). In the CASSCF wavefunctions of the $1^2A''$, $1^2A'$, and $2^2A''$ ionic states, we find the dominant configurations of $(3a'')^{-1}$, $(13a')^{-1}$, and $(2a'')^{-1}$, respectively (see the electron configuration of the ground-state molecule in section of calculation details). The 3a″ molecular orbital (MO) is a π orbital at the C═C bond with some C−Cl antibonding. Removal of one electron from the 3a″ MO will lead to elongation of the C−C bond and shortening of the C−Cl bond, which explains the changes in the $1^2A''$ geometry compared to the geometry of the molecule (see Table 1). The 13a′ MO is mainly characterized by the chlorine 3p nonbonding orbitals in the molecular plane. Removal of one electron from the 13a′ MO will not lead to significant bond elongation or shortening, and we note in Table 1 that the C_1-C_2 and C_2-Cl bond length values in the $1^2A'$ geometry are similar to the respective values in the geometry of the molecule. The 2a″ MO is a delocalized π orbital with bonding at both the C−C and C−Cl bonds, but the contribution from the chlorine 3p orbital is the most important. Removal of one electron from the 2a″ MO will lead to elongation of the C−C and C−Cl bonds, which explains the fact that the geometry of the $2^2A''$ ionic state has a longer C_1-C_2 bond and a much longer C_2-Cl bond than the geometry of the molecule (see Table 1).

CASPT2 Excitation Energies. In Table 2 given are the CASPT2 T_0, T_v, and T_v' values for the $1^2A''$, $1^2A'$, $2^2A''$, and $2^2A'$ states of the $C_2H_3Cl^+$ ion. The CASPT2 T_0, T_v, and T_v' calculations predict the same energy ordering for the four ionic states and the calculations indicate that the $1^2A''$, $1^2A'$, $2^2A''$, and $2^2A'$ states are the X, A, B, and C states of the ion, respectively, in line with the previous assignments.[3,5−9]

The CASPT2 T_0 value of 1.67 eV for the $1^2A'$ state is very close to the experimental value of 1.72 eV for the A state.[6] The CASPT2 T_v values (no available experimental data) for the $1^2A'$, $2^2A''$, and $2^2A'$ states are slightly different from the previously calculated values (listed in Table 2) using the TDDFT method[5] (the discrepancies being smaller than 0.25 eV). The CASPT2 T_v' values of 1.55 and 2.93 eV for the $1^2A'$ and $2^2A''$ states are very close to the experimental values (1.54 and 2.96 eV, respectively) evaluated using the VIE values reported in ref 6 and in reasonable agreement with the experimental values (1.66 and 3.13 eV, respectively) evaluated using the VIE values reported in ref 7. The CASPT2 T_v' value of 3.53 eV for the $2^2A'$ state is very close to the experimental value (3.56 eV) evaluated using the VIE values reported in ref 7 and in reasonable agreement with the experimental value (3.38 eV) evaluated using the VIE values reported in ref 6.

TABLE 2: CASPT2 Adiabatic (T_0) and Vertical (T_v) Excitation Energy Values (in eV) for the $1^2A''$, $1^2A'$, $2^2A''$, and $2^2A'$ States of the $C_2H_3Cl^+$ Ion and CASPT2 Relative Energies (T_v') Values (in eV) of the Four Ionic States at the Experimental Geometry of the Ground-State C_2H_3Cl Molecule, Together with Available Experimental T_0 and T_v' Values and the Previously Reported TDDFT T_v Values

	T_0		T_v		T_v'		
	CASPT2	exptl[a]	CASPT2	TDDFT[b]	CASPT2	exptl[a]	exptl[c]
$1^2A''$	0.0	0.0	0.0	0.0	0.0	0.0	0.0
$1^2A'$	1.67	1.72	1.83	1.76	1.55	1.54	1.66
$2^2A''$	2.71		3.49	3.71	2.93	2.96	3.13
$2^2A'$	*d*		4.15	3.91	3.53	3.38	3.56

[a] Reference 6. [b] TDDFT/UB3LYP/6-311++G** calculations; ref 5. [c] He(I)/He(II) PES; ref 7. [d] Our calculations indicate that the $2^2A'$ state is repulsive.

TABLE 3: Oscillator Strength *f* Values for the Vertical Excitations from the $1^2A''$ (X^2A'') and $1^2A'$ (A^2A') States (at the Respective CASPT2 Optimized Geometries) Calculated Using the CASSCF State Interaction Method and the CASPT2 Energy Differences

transition	CASPT2 T_v	*f*	*f*[a]
A^2A' ($1^2A'$) ← X^2A''($1^2A''$)	1.83	1.60×10^{-7}	0.000027
B^2A'' ($2^2A''$) ← X^2A''	3.49	0.036652	0.043708
C^2A' (C^2A') ← X^2A''	4.15	0.000828	0.000131
B^2A'' ← A^2A'	1.34[b]	0.000003	0.000021
C^2A' ← A^2A'	1.94[b]	0.000048	0.003441
X^2A'' ← A^2A'	−1.44	0.000005	0.000015[c]

[a] The *f* values calculated using TDDFT/UB3LYP method, reported in ref 5. [b] The CASPT2 vertical excitation energy from the $1^2A'$ (A^2A') state. [c] The *f* values calculated using TDDFT/UB3LYP method, reported in ref 3.

CASSCF//CASPT2 Oscillator Strength *f* Values. We used the CASSCF state interaction (CASSI) method[34,35] to compute the oscillator strength *f* values, using energy differences corrected by the CASPT2 calculations, for the vertical transitions from the $1^2A''$ (X^2A'') and $1^2A'$ (A^2A') states (at their respective CASPT2 geometries). The computed oscillator strength *f* values are given in Table 3.

Our calculations predict small *f* values (smaller than 10^{-3}) for the A^2A' ($1^2A'$) ← X^2A'' ($1^2A''$) and C^2A' ($2^2A'$) ← X^2A'' transitions and a large *f* value (0.036652) for the B^2A'' ($2^2A''$) ← X^2A'' transition, as the previous TDDFT/UB3LYP calculations[5] (see Table 3). Our calculations predict small *f* values for the B^2A'' ← A^2A' and C^2A' ← A^2A' transitions. The previous TDDFT/UB3LYP calculations[5] predicted a small *f* value for the

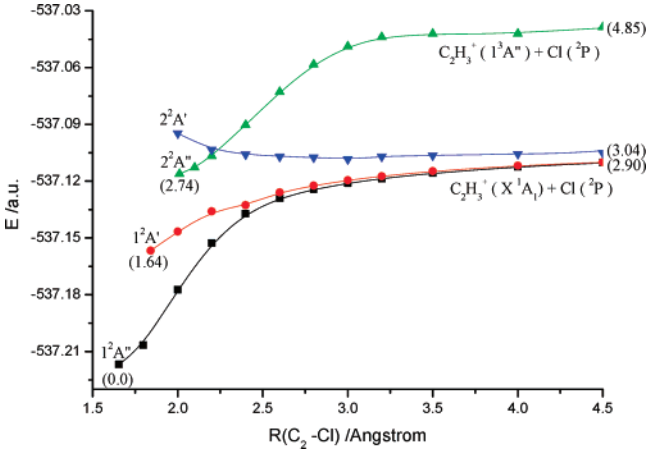

Figure 2. CASPT2//CASSCF potential energy curves for Cl-loss dissociation from the $1^2A''$ (X^2A''), $1^2A'$, $2^2A''$, and $2^2A'$ states of the $C_2H_3Cl^+$ ion. The values given in parentheses are the CASPT2//CASSCF relative energies (in eV) of the reactants and asymptote products to the ground-state reactant.

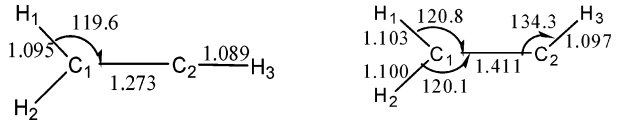

Figure 3. CASSCF optimized geometries of $C_2H_3^+$ (X^1A_1) (a) and $C_2H_3^+$ ($1^3A''$) (b).

$B^2A'' \leftarrow A^2A'$ transition, and a relatively large f value (0.003 441) for the $C^2A' \leftarrow A^2A'$ transition. We also calculated the f value for the $X^2A'' \leftarrow A^2A'$ transition, and the calculated f value is very small (5×10^{-6}), which is compatible to the experimental fact that the A state has a long lifetime.[3]

CASPT2//CASSCF Cl-Loss Dissociation Potential Energy Curves. In Figure 2 shown are the CASPT2//CASSCF Cl-loss dissociation PECs for the $1^2A''$ (X^2A''), $1^2A'$ (A^2A'), $2^2A''$ (B^2A''), and $2^2A'$ (C^2A') states of the $C_2H_3Cl^+$ ion, and the CASPT2//CASSCF relative energies for the reactants and asymptote products of the four states to the ground-state reactant are given in parentheses.

Very small charge values (<0.008 e) at the Cl atom in the asymptote products indicate that the dissociation products for the four states are the neutral Cl atom plus the $C_2H_3^+$ ion in different states. We then performed CAS calculations (using the full valence active space) for the 1^1A_1 state (X^1A_1 with an electronic configuration of $(1a_1)^2(2a_1)^2(3a_1)^2(4a_1)^2(5a_1)^2(1b_2)^2(1b_1)^2$, C_{2v}) and the $1^3A''$ state (the lowest-lying triplet state with an electronic configuration of $(1a')^2(2a')^2(3a')^2(4a')^2(5a')^2(6a')^2(1a'')^1(7a')^1$, C_s) of the $C_2H_3^+$ ion. The CASPT2//CASSCF relative energy (T_0) value for $1^3A''$ to 1^1A_1 is evaluated to be 1.88 eV.

The $1^2A''$, $1^2A'$, and $2^2A'$ asymptote products have similar CASPT2//CASSCF energy values (the discrepancies being smaller than 0.15 eV) and the geometries of the C_2H_3 fragment in the three asymptote products are close to the CASSCF geometry of the X^1A_1 state of the $C_2H_3^+$ ion (see Figure 3a). We conclude that the Cl-loss dissociation products of the $1^2A''$ (X^2A''), $1^2A'$ (A^2A'), and $2^2A'$ (C^2A') states of the $C_2H_3Cl^+$ ion are all [$C_2H_3^+$ (X^1A_1) + Cl (^2P)]. The $2^2A''$ asymptote product is higher in the CASPT2//CASSCF energy than the $1^2A''$ asymptote product by 1.95 eV, which is very close to the CASPT2//CASSCF T_0 value of 1.88 eV for the $1^3A''$ state of $C_2H_3^+$, and the geometry of the C_2H_3 fragment in the $2^2A''$ asymptote product is close to the CASSCF geometry of the $1^3A''$ state of the $C_2H_3^+$ ion (see Figure 3b). We conclude that the Cl-loss dissociation products of the $2^2A''$ (B^2A'') state of the $C_2H_3Cl^+$ ion are [$C_2H_3^+$ ($1^3A''$) + Cl (^2P)].

We performed the CASPT2 geometry optimization calculations for the 1^1A_1 (X^1A_1) and $1^3A''$ states of the $C_2H_3^+$ ion. On the basis of the CASPT2 energetic results for the 1^1A_1 and $1^3A''$ states of the $C_2H_3^+$ ion, the Cl (^2P) atom, the $1^2A''$, $1^2A'$, and $2^2A''$ states of the $C_2H_3Cl^+$ ion, and the ground-state C_2H_3Cl molecule, we evaluated the CASPT2 D_0 values and CASPT2 AE (appearance energy for production of $C_2H_3^+$ from the ground-state C_2H_3Cl molecule) values. The CASPT2 D_0 values are 2.94 eV for the $C_2H_3Cl^+$ (X^2A'') $\rightarrow$ $C_2H_3^+$ (X^1A_1) + Cl (^2P) dissociation, 1.27 eV for the $C_2H_3Cl^+$ (A^2A') $\rightarrow$ $C_2H_3^+$ (X^1A_1) + Cl (^2P) dissociation, and 2.11 eV for the $C_2H_3Cl^+$ (B^2A'') $\rightarrow$ $C_2H_3^+$ ($1^3A''$) + Cl (^2P) dissociation. The CASPT2 AE values for the $C_2H_3^+$ (X^1A_1) and $C_2H_3^+$ ($1^3A''$) ions are 12.79 and 14.67 eV, which are in good agreement with the experimental values (reported by Sheng et al.[11]) of 12.54 and 14.82 eV, respectively. The (estimated) experimental D_0 value[11] of 2.56 eV for the $C_2H_3Cl^+$ (X^2A'') $\rightarrow$ $C_2H_3^+$ (X^1A_1) + Cl (^2P) dissociation is significantly smaller than our CASPT2 value of 2.94 eV.

As shown in Figure 2, the energy monotonically increases with the $R(C_2-Cl)$ value along the $1^2A''$, $1^2A'$, and $2^2A''$ PECs but monotonically decreases along the $2^2A'$ PEC. As expected by Kim et al.,[5] the B^2A'' ($2^2A''$) state is a bound state and the C^2A' ($2^2A'$) state is repulsive. The $2^2A''$ and $2^2A'$ PECs cross at $R(C_2-Cl) \approx 2.24$ Å in Figure 2, and the B/C cross was also expected by Kim et al.[5]

Discussion on Photodissociation of $C_2H_3Cl^+$ to $C_2H_3^+$. We first present a discussion on the proposed mechanism of Kim et al.[5] for the photodissociation of the X^2A'' state of the $C_2H_3Cl^+$ ion at 357 nm (3.47 eV) generating the $C_2H_3^+$ ion. Because the CASPT2 T_v value of 3.49 eV (see Table 2) for the $2^2A''$ (B^2A'') state is almost equal to the experimental photon energy value of 3.47 eV (357 nm) and the computed oscillator strength f value for the $B^2A'' \leftarrow X^2A''$ transition is large (see Table 3), a transition of the X^2A'' state to the B^2A'' state is possible. The CASPT2//CASSCF energy at the B/C PEC crossing point in Figure 2 is about 3.08 eV higher than the CASPT2//CASSCF energy of the X^2A'' reactant (the minimum point along the crossing seam between the B^2A'' and C^2A' potential energy surfaces would have a relative energy value slightly smaller than 3.08 eV). Because the transition of the X^2A'' state to the B^2A'' state is possible and the relative energy at the B/C crossing point to the X^2A'' reactant is smaller than 3.47 eV (357 nm), the following photodissociation process for the X^2A'' state of the $C_2H_3Cl^+$ ion at 357 nm is suggested: the X^2A'' state undergoes transition to the B^2A'' state followed by predissociation of the B^2A'' state by the repulsive C^2A' state (via the B/C crossing) leading to the $C_2H_3^+(X^1A_1)$ ion. This photodissociation process was just the proposed main reaction pathway of the X^2A'' state at 357 nm by Kim et al.[5] based on their experimental data. There is also a possibility that, after the excitation of the X^2A'' state to B^2A'', the $C_2H_3Cl^+$ (B^2A'') ion undergoes radiationless decay to the X^2A'' state followed by the dissociation on the X^2A'' state.

The $A^2A' \leftarrow X^2A''$ transition is unlikely because the f value is very small. The $C^2A' \leftarrow X^2A''$ transition is also unlikely because the f value is small and the (CASPT2) T_v value of 4.15 eV (see Table 2) for the $2^2A'$ (C^2A') state is larger than 3.47 eV (357 nm). Therefore, photodissociation of the X^2A'' state via the A^2A' or C^2A' state is unlikely. On the basis of the

CASPT2 energy values for the $1^3A''$ state of the $C_2H_3^+$ ion, the Cl (^2P) atom, and the X^2A'' state of the $C_2H_3Cl^+$ ion, the CASPT2 relative energy value for $C_2H_3^+$ ($1^3A''$) + Cl [the $2^2A''$ (B^2A'') dissociation products, see Figure 2] to the X^2A'' reactant is evaluated to be 4.82 eV (the CASPT2//CASSCF relative energy value being 4.85 eV, see Figure 2), which is larger than the experimental photon energy value of 3.47 eV (357 nm). Therefore, we consider that photodissociation of the X^2A'' state via the $B^2A'' \leftarrow X^2A''$ transition followed by a direct dissociation of B^2A'' to $C_2H_3^+$ ($1^3A''$) is not possible.

We will also present preliminary discussion on some other proposed mechanisms of Kim et al.[5] concerning dissociation of the $C_2H_3Cl^+$ ion generating the $C_2H_3^+$ ion. Kim et al.[5] reported that the $C_2H_3Cl^+$ ion in the ground state did not undergo dissociation at 514.5 nm (2.41 eV), 488.0 nm (2.54 eV), or 476.5 nm (2.60 eV), though the average internal energy value of 2.59, 2.72, or 2.78 eV (the photon energy value added by a value of 0.18 eV, see ref 5) exceeded the (estimated) experimental D_0 value of 2.56 eV[11] for the ground state. Our CASPT2 calculations have predicted a D_0 value of 2.94 eV (see the last subsection) for the ground state, which is larger than the three average internal energy values, and therefore our CASPT2 calculations support the experimental facts that the $C_2H_3Cl^+$ ion in the ground state did not undergo dissociation in the visible spectral region. Kim et al.[5] reported photodissociation processes for the A state of the $C_2H_3Cl^+$ ion to $C_2H_3^+$ at 514.5 nm (2.41 eV) and 357 nm (3.47 eV), and they proposed that the $C^2A' \leftarrow A^2A'$ optical transition was responsible for the photodissociation processes. Because our computed f values (see Table 3) for the $C^2A' \leftarrow A^2A'$ and $B^2A'' \leftarrow A^2A'$ transitions are small, we presumably consider that the probability for photodissociation of the A^2A' state via C^2A' or B^2A'' is small. Our CASPT2 calculations have predicted a small D_0 value of 1.27 eV (see the last subsection) for the A^2A' state, and the calculations imply that a direct dissociation of the A state to $C_2H_3^+(X^1A_1)$ is energetically feasible.

Conclusions

The $C_2H_3Cl^+$ ion is the smallest among the molecular ions having long-lived excited electronic states observed recently by Kim et al. We studied the $1^2A''$ (X^2A''), $1^2A'$ (A^2A'), $2^2A''$ (B^2A''), and $2^2A'$ (C^2A') states of the $C_2H_3Cl^+$ ion using the CASSCF and CASPT2 methods. Our energetic calculations support the previous assignments for the four ionic states. The computed oscillator strength f value for the $X^2A'' \leftarrow A^2A'$ transition is very small, which is in line with the experimental fact that the A state has a long lifetime. The CASPT2 geometry and T_0 value for the A^2A' state are in good agreement with experiment. The CASPT2 T_v' values for the three excited states are in good agreement with the values evaluated using the experimental VIEs.

The Cl-loss dissociation PEC calculations at the CASPT2//CASSCF level predict that the X^2A'', A^2A', and C^2A' states of $C_2H_3Cl^+$ correlate to $C_2H_3^+$ (X^1A_1) and the B^2A'' state correlates to $C_2H_3^+$ ($1^3A''$). The CASPT2 D_0 values for the (adiabatic) dissociations of the X^2A'', A^2A', and B^2A'' states of $C_2H_3Cl^+$ and the CASPT2 AE values for $C_2H_3^+$ (X^1A_1) and $C_2H_3^+$ ($1^3A''$) were evaluated, and the calculated AE values are in good agreement with experiment. Along the $1^2A''$, $1^2A'$, and $2^2A''$ PECs the energy monotonically increases with the $R(C_2-Cl)$ value, and along the $2^2A'$ PEC the energy monotonically decreases. As expected by Kim et al., the B^2A'' ($2^2A''$) state is a bound state and the C^2A' ($2^2A'$) state is repulsive. The B^2A'' and C^2A' PECs cross at $R(C_2-Cl) \approx 2.24$ Å, and the CASPT2//CASSCF relative energy at the "crossing point" to the X^2A'' reactant is about 3.08 eV. The B/C crossing was also expected by Kim et al.

We present discussions on mechanisms for the photodissociation of the $C_2H_3Cl^+$ ion generating the $C_2H_3^+$ ion on the basis of our calculated energetic results and oscillator strength f values. Because the transition of the X^2A'' state to the B^2A'' state is possible and the relative energy at the B/C crossing point to the X^2A'' reactant is smaller than 3.47 eV (357 nm), the following photodissociation process for the X^2A'' state of the $C_2H_3Cl^+$ ion at 357 nm is suggested: the X^2A'' state undergoes transition to the B^2A'' state followed by predissociation of the B^2A'' state by the repulsive C^2A' state (via the B/C crossing) leading to the $C_2H_3^+(X^1A_1)$ ion. This photodissociation process was just the proposed main reaction pathway of the X^2A'' state at 357 nm by Kim et al.[5] based on their experimental data. Our calculation results indicate that photodissociation of the X^2A'' state via the A^2A' or C^2A' state is unlikely and that photodissociation of the X^2A'' state via the $B^2A'' \leftarrow X^2A''$ transition followed by a direct dissociation of B^2A'' to $C_2H_3^+$ ($1^3A''$) is not possible either. Our CASPT2 calculations support the experimental facts that the $C_2H_3Cl^+$ ion in the ground state did not undergo dissociation in the visible spectral region. On the basis of our calculation results, we consider that the probability for the photodissociation of the A^2A' state via C^2A' or B^2A'' is small (the experimental workers proposed that the $C^2A' \leftarrow A^2A'$ optical transition was responsible for the photodissociation of the A state) and suggest that a direct dissociation of the A state to $C_2H_3^+(X^1A_1)$ is energetically feasible.

Acknowledgment. We appreciate the financial support of this work that was provide by National Natural Science Foundation of China through Contract Nos. 20333050, 20673142, and 20773161, and the Natural Science Foundation of Hebei Province through Contract No. B2006000137.

Supporting Information Available: CASSCF geometries of the ionic states. This material is available free of charge via the Internet at http://pubs.acs.org.

References and Notes

(1) Kim, M. S.; Kwon, C. H.; Choe, J. C. *J. Chem. Phys.* **2000**, *113*, 9532−9539.
(2) Youn, Y. Y.; Kwon, C. H.; Choe, J. C.; Kim, M. S. *J. Chem. Phys.* **2002**, *117*, 2538−2545.
(3) Youn, Y. Y.; Choe, J. C.; Kim, M. S. *J. Am. Soc. Mass Spectrom.* **2003**, *14*, 110−116.
(4) Lee, M.; Kim, M. S. *J. Phys. Chem. A* **2006**, *110*, 9377−9382.
(5) Yoon, S. H.; Choe, J. C.; Kim, M. S. *Int. J. Mass Spectrom.* **2003**, *227*, 21−32.
(6) Lake, R. F.; Thompson, S. H. *Proc. R. Soc. London A* **1970**, *315*, 323−338.
(7) Locht, R.; Leyh, B.; Hottmann, K.; Baumgärtel, H. *Chem. Phys.* **1997**, *220*, 217−232.
(8) Sze, K. H.; Brion, C. E.; Katrib, A.; El-Issa, B. *Chem. Phys.* **1989**, *137*, 369−390.
(9) Niessen, W. V.; Åsbrink, L.; Bieri, G. *J. Electron. Spectrosc. Relat. Phenom.* **1982**, *26*, 173−201.
(10) Chang, J.-L.; Shieh, J.-C.; Wu, J.-C.; Li, R.; Chen, Y.-T. *Chem. Phys. Lett.* **2000**, *325*, 369−374.
(11) Sheng, L.; Qi, F.; Tao, L.; Zhang, Y.; Yu, S.; Wong, C.-K.; Li, W.-K. *Int. J. Mass Spectrom. Ion Processes* **1995**, *148*, 179−189.
(12) Hughes, B. M.; Tiernan, T. O.; Futrell, J. H. *J. Phys. Chem.* **1969**, *73*, 829−840.
(13) Reinke, D.; Kraessig, R.; Baumgärtel, H. *Z. Naturforsch.* **1973**, *28a*, 1021−1031.
(14) Sood, S. P.; Watanabe, K. *J. Chem. Phys.* **1966**, *45*, 2913−2915.
(15) Locht, R.; Leyh, B.; Hottmann, K.; Baumgärtel, H. *Chem. Phys.* **1997**, *220*, 207−216.
(16) Wittel, K.; Bock, H. *Chem. Ber.* **1974**, *107*, 317−338.

(17) Farmanara, P.; Stert, V.; Radloff, W. *Chem. Phys. Lett.* **1998**, *288*, 518−522.
(18) Zhang, Y.; Sheng, L.; Qi, F.; Gao, H.; Yu, S. *J. Electron. Spectrosc. Relat. Phenom.* **1996**, *79*, 483−485.
(19) Roos, B. O. *Adv. Chem. Phys.* **1987**, *69*, 399−445.
(20) Andersson, K.; Roos, B. O. *Int. J. Quantum Chem.* **1993**, *45*, 591−607.
(21) Andersson, K.; Malmqvist, P.; Roos, B. O. In *Modern Electronic Structure Theory*; Yarkony, D. R., Ed.; World Scientific: Singapore, 1995; Part 1, p 55.
(22) Andersson, K.; et al. MOLCAS (version 5.4), University of Lund, Sweden, 2002.
(23) Andersson, K.; et al. MOLCAS (version 6.2), University of Lund, Sweden, 2005.
(24) Almlof, J.; Taylor, P. R. *J. Chem. Phys.* **1987**, *86*, 4070−4077.
(25) Widmark, P.-O.; Malmqvist, P.-A.; Roos, B. O. *Theor. Chim. Acta* **1990**, *77*, 291−306.
(26) Widmark, P.-O.; Persson, B.-J.; Roos, B. O. *Theor. Chim. Acta* **1991**, *79*, 419−432.
(27) Xi, H.-W.; Huang, M.-B. *J. Phys. Chem. A* **2006**, *110*, 8167−8173.
(28) Chen, B.-Z.; Chang, H.-B.; Huang, M.-B. *J. Chem. Phys.* **2006**, *125*, 054310.
(29) Yu, S.-Y.; Huang, M.-B.; Li, W.-Z. *J. Phys. Chem. A* **2006**, *110*, 1078−1083.
(30) Liu, T.; Huang, M.-B.; Xi, H.-W. *Chem. Phys.* **2007**, *332*, 277−283.
(31) Xi, H.-W.; Huang, M.-B. *Chem. Phys. Lett.* **2006**, *430*, 227−234.
(32) Xi, H.-W.; Huang, M.-B. *Chem. Phys. Lett.* **2006**. *425*, 28−34.
(33) Herzberg, G. *Electronic spectra and electronic structure of polyatomic molecules*; Van Nostrand: New York, 1966.
(34) Malmqvist, P.-Å. *Int. J. Quantum Chem.* **1986**, *30*, 479−494.
(35) Malmqvist, P.-Å.; Roos, B. O. *Chem. Phys. Lett.* **1989**, *155*, 189−194.